Rapid Communications | Editors' Suggestion

$\mathbb{Z}_4$ parafermions in one-dimensional fermionic lattices

Alessio Calzona,[1,2,*] Tobias Meng,[3] Maura Sassetti,[2] and Thomas L. Schmidt[1]
[1]*Physics and Materials Science Research Unit, University of Luxembourg, L-1511, Luxembourg*
[2]*Dipartimento di Fisica, Università di Genova and SPIN-CNR, Via Dodecaneso 33, I-16146 Genova, Italy*
[3]*Institut für Theoretische Physik, Technische Universität Dresden, D-01062 Dresden, Germany*

(Received 16 February 2018; revised manuscript received 8 October 2018; published 14 November 2018)

Parafermions are emergent excitations which generalize Majorana fermions and are potentially relevant to topological quantum computation. Using the concept of Fock parafermions, we present a mapping between lattice $\mathbb{Z}_4$ parafermions and lattice spin-1/2 fermions which preserves the locality of operators with $\mathbb{Z}_4$ symmetry. Based on this mapping, we construct an exactly solvable, local, and interacting one-dimensional fermionic Hamiltonian which hosts zero-energy modes obeying parafermionic algebra. We numerically show that this parafermionic phase remains stable in a wide range of parameters, and discuss its signatures in the fermionic spectral function.

DOI: 10.1103/PhysRevB.98.201110

Introduction. In its early years, the field of topological states of matter has mainly been centered around noninteracting Hamiltonians and the topology of their band structures [1–4]. In electronic systems, however, the presence of Coulomb repulsion raises the question to which degree topology and interactions coexist or compete. It has by now become clear that there is no general answer to this question—the effect of interactions can range from perturbatively small modifications of effective band structures to a complete loss of the topological distinction between different phases. As a third and much more exciting option, interactions can give rise to entirely new phases of matter, a prime example of which are topologically ordered states such as fractional quantum Hall states. These systems feature emergent low-energy excitations called anyons that behave differently from fermions or bosons [5]. The most sought after are non-Abelian anyons in many-particle systems with a topologically protected ground-state degeneracy. Braiding two of these non-Abelian anyons implements a rotation in the degenerate ground-state manifold, which in turn allows one to perform quantum computation in a way that minimizes decoherence at the hardware level [5–7].

As a major breakthrough, it has been realized that anyonic excitations can not only exist as quasiparticles of strongly interacting systems such as fractional quantum Hall states, but may also emerge as special bound states of quadratic Hamiltonians. The best-studied examples here are Majorana fermions, which appear as vortex-bound states in p-wave superconductors [8], and at domain walls of simple chains of superconducting spinless electrons [9,10]. A large body of research has been devoted to the experimental realization of Majorana bound states, including in particular semiconducting quantum wires with strong spin-orbit coupling [11–16] or magnetic adatoms on superconductors [17–22]. While Majorana fermions are the simplest example of non-Abelian anyons, they are not complex enough to implement universal quantum computing. More recently, the focus has thus shifted to so-called $\mathbb{Z}_n$ parafermions, generalizations of Majorana fermions associated with richer braiding properties [5,23].

These more complicated parafermions cannot be realized in noninteracting Hamiltonians, but rather are an example of a topological phenomenon that only exists in the presence of electron-electron interactions. Various experimental realizations for some of those parafermions have been proposed, for instance, quantum spin Hall systems [24–28], quantum wires [27,29–31], fractional quantum Hall insulators [32–39], and other systems [40,41]. These theoretical studies, however, are all based on effective low-energy field theories and extensions of Luttinger liquid physics. Hence, the parafermions they predict are not exact eigenstates of a microscopic fermionic Hamiltonian. A complementary line of research has been devoted to more mathematical studies of intrinsic properties of parafermions chains [42–51]. In the present Rapid Communication, we propose an exact mapping between parafermionic chains and electronic Hamiltonians on a lattice. This mapping not only provides an insightful bridge between mathematical models and physical systems, but also paves the way for the systematic implementation and analysis of parafermionic Hamiltonians using fermions.

From parafermions to fermions. The starting point of our analysis is a one-dimensional chain of $\mathbb{Z}_4$ parafermions, which is a natural generalization of the Kitaev chain of Majorana fermions. At each site $i \in \{1, \ldots, L\}$, we define two parafermionic operators a_i and b_i, which satisfy $a_i^4 = 1$ and $a_i^3 = a_i^\dagger$ (the same applies for b_i). By definition, parafermionic operators satisfy the anyonic exchange statistic: $a_l a_j = i\, a_j a_l$, $b_l b_j = i\, b_j b_l$ for $l < j$, and $a_l b_j = i\, b_j a_l$ for $l \leqslant j$. To relate these operators to physical electrons, we study how they act on the states of the system. The fact that $a_i^4 = 1 = b_i^4$ implies that each lattice site can be associated with four different states, and that the application of the operators a_i and b_i cycles through those states. This notion can be made more precise by associating a Fock space to the parafermionic operators

*calzona@fisica.unige.it

via the introduction of "Fock parafermions" (FPFs) [52,53]. The latter are described by creation ($d_j^\dagger$) and annihilation (d_j) operators, which allow us to express a_i and b_i as

$$a_j = d_j + d_j^{\dagger 3}, \quad b_j = e^{i\pi/4}\left(d_j i^{N_j} + d_j^{\dagger 3}\right), \tag{1}$$

where $N_j = \sum_{m=1}^{3} d_j^{\dagger m} d_j^m$ is the number operator for FPF whose four integer eigenvalues run from 0 to 3. The parafermionic algebra of a_i and b_i is handed down to the FPFs in their commutations relations: $d_l d_j = i\, d_j d_l$ and $d_j d_l^\dagger = i\, d_l^\dagger d_j$ for $l < j$. Moreover, on a given site one has $d_j^{\dagger m} d_j^m + d_j^{(4-m)} d_j^{\dagger(4-m)} = 1$, for $m = 1, 2, 3$, and $d_j^4 = 0$.

The single-site four-dimensional parafermionic Fock space can be identified with the Fock space of spin-1/2 fermions, inducing an on-site mapping between FPF operator and physical fermions. The introduction of appropriate string factors allows one to extend the mapping over the whole chain, in analogy with the well-known Jordan-Wigner transformation between spin chains and fermionic ones. Since the identification between the two Fock spaces is not unique, one can find many different mappings between FPFs and fermions on a lattice. Here, we consider in particular the following one (derived in the Supplemental Material [53]),

$$\begin{aligned} d_j = {} & i^{\sum_{p<j}(n_{p\downarrow}+3n_{p\uparrow}-2n_{p\uparrow}n_{p\downarrow})} \\ & \times (c_{j\uparrow} - c_{j\uparrow}n_{j\downarrow} - c_{j\uparrow}^\dagger n_{j\downarrow} + i c_{j\downarrow} n_{j\uparrow}), \end{aligned} \tag{2}$$

which features a definite odd fermion parity ($n_{j\sigma} = c_{j\sigma}^\dagger c_{j\sigma}$). This property is crucial since it remarkably ensures that every local parafermionic operator which conserves the number of FPFs modulo 4 is transformed into a fermionic operator *without* string factors [53]. Despite the high nonlocality of Eq. (2), it is therefore possible to map parafermionic nearest-neighbor Hamiltonians into fermionic models with on-site and nearest-neighbor terms only.

Mapping of the Hamiltonian. In the remainder, we apply the above mapping to the following $\mathbb{Z}_4$-parafermionic Hamiltonian on an open L-site chain [47],

$$H_J = -J e^{i\frac{\pi}{4}} \sum_{j=1}^{L-1} b_j a_{j+1}^\dagger + \text{H.c.}, \tag{3}$$

where we assume $J > 0$. This exactly solvable model [42,53] can be seen as a generalization of Kitaev's Majorana chain model and has a nontrivial topology. There are two dangling parafermions, a_1 and b_L, which commute with the Hamiltonian and induce an exact and topologically protected fourfold degeneracy throughout the entire spectrum. As one important feature, the Hamiltonian H_J has a $\mathbb{Z}_4$ symmetry $\mathcal{Z} = i^{\sum_j N_j}$ which guarantees the conservation modulo 4 of the total number of FPFs.

The mapping (2) allows us to translate the Hamiltonian (3) to a local fermionic Hamiltonian $H_J = H^{(2)} + H^{(4)} + H^{(6)}$, with

$$H^{(2)} = -J \sum_{\sigma,j} [c_{\sigma,j}^\dagger c_{\sigma,j+1} - i\, c_{-\sigma,j}^\dagger c_{\sigma,j+1}^\dagger] + \text{H.c.}, \tag{4}$$

$$\begin{aligned} H^{(4)} = {} & -J \sum_{\sigma,j} [c_{\sigma,j}^\dagger c_{\sigma,j+1}(-n_{-\sigma,j} - n_{-\sigma,j+1}) \\ & + c_{\sigma,j}^\dagger c_{-\sigma,j+1}\, i(n_{-\sigma,j} + n_{\sigma,j+1}) \\ & + c_{-\sigma,j}^\dagger c_{\sigma,j+1}^\dagger\, i(n_{\sigma,j} + n_{-\sigma,j+1}) \\ & + c_{\sigma,j}^\dagger c_{\sigma,j+1}^\dagger (n_{-\sigma,j} - n_{-\sigma,j+1})] + \text{H.c.}, \end{aligned} \tag{5}$$

$$\begin{aligned} H^{(6)} = {} & -J \sum_j [-2i\, c_{\sigma,j}^\dagger c_{-\sigma,j+1}(n_{-\sigma,j} n_{\sigma,j+1}) \\ & - 2i\, c_{-\sigma,j}^\dagger c_{\sigma,j+1}^\dagger (n_{\sigma,j} n_{-\sigma,j+1})] + \text{H.c.} \end{aligned} \tag{6}$$

In the fermionic language, H_J consists of superconducting pairing and hopping terms with and without spin flip, locally weighted by the fermion occupation numbers on the lattice sites. Note that the Hamiltonian H_J is time-reversal invariant.

The mapping we have developed allows us to express parafermionic operators in terms of electrons. The zero-energy parafermionic modes, in particular, have the following fermionic expression,

$$\begin{aligned} a_1 = {} & i c_{1\downarrow} n_{1\uparrow} - c_{1\uparrow}^\dagger n_{1\downarrow} + c_{1\uparrow}(1 - n_{1\downarrow}) + i c_{1\downarrow}^\dagger (1 - n_{1\uparrow}), \\ b_L = {} & e^{i\pi/4}(-i)^{\sum_{j=1}^{L-1} N_j} [i c_{L\uparrow}^\dagger n_{L\downarrow} + i c_{L\uparrow}(1 - n_{L\downarrow}) \\ & - i c_{L\downarrow}^\dagger (1 - n_{L\uparrow}) - i c_{L\downarrow} n_{L\uparrow}]. \end{aligned} \tag{7}$$

These equations represent an important result, namely, the explicit expression of combinations of fermionic operators that satisfy the parafermionic algebra and that commute with the fermionic Hamiltonian H_J.

An important question concerns the locality and topological protection of the zero-energy states of the fermionic Hamiltonian. Although a_1 and b_L are localized at the edge in the parafermionic language, one of the corresponding fermionized operators (in our case b_L) inevitably contains a nonlocal string factor. This string factor is not associated with a density of states (see below), but allows the edge mode to "feel" what happens in the bulk. The nonlocality hence challenges the *topological* protection of the fourfold ground-state degeneracy in the fermionic model. As we will discuss in the next section, it indeed turns out that only a twofold degeneracy is topologically protected. Remarkably, the nonlocality of b_L does not prevent us from finding local operators on either edge of the fermionic chain that cycle through the four degenerate ground states (see Supplemental Material [53]).

Topological properties of the fermionic chain. In the parafermionic language, the model in Eq. (3) represents a topological phase [45–47] in which the spectrum exhibits a topologically protected fourfold degeneracy that cannot be lifted by local parafermionic perturbations. It is natural to ask if the same holds also for the corresponding fermionic chain, since it is well known that the presence of string factors can change the topological properties of the system. The prototypical example is the Kitaev chain, which is related by a nonlocal Jordan-Wigner transformation to the topologically trivial quantum Ising model [9].

In this respect, it is instructive to study the symmetries featured by the fermionic model in Eqs. (4)–(6). The $\mathbb{Z}_4$ symmetry of the parafermionic Hamiltonian in Eq. (3) can be expressed in terms of fermions as $\mathcal{Z} = i^{\sum_j [(n_{j\uparrow}+n_{j\downarrow})^2 + 2n_{j\downarrow}]}$. Its square corresponds to the usual $\mathbb{Z}_2$ fermion parity $\mathcal{P} = \mathcal{Z}^2 = (-1)^{\sum_j (n_{j\uparrow}+n_{j\downarrow})}$. Interestingly, the local operator

$M_j = i\gamma_{\uparrow,j}\gamma_{\downarrow,j}$, where $\gamma_{\sigma,j} = c^\dagger_{\sigma,j} + c_{\sigma,j}$ are Majorana operators, commutes with the Hamiltonian but anticommutes with the $\mathbb{Z}_4$ symmetry $\{M_j, \mathcal{Z}\} = 0$. It can be therefore identified as a $\mathbb{Z}_2$ local order operator, associated with the $\mathbb{Z}_2$ symmetry $\mathcal{S}_B = e^{-i\frac{\pi}{4}} 2^{-\frac{1}{2}} \mathcal{Z} + \text{H.c.}$ which is spontaneously broken and satisfies $[\mathcal{S}_B, H_J] = \{\mathcal{S}_B, M_j\} = 0$. This local order parameter thus differentiates the four degenerate ground states into two pairs and the degeneracy between them can be split by a local perturbation containing any of the M_j. A concrete example of such a perturbation is a magnetic field along the y axis,

$$H_y = B_y \sum_{i=1}^{L} i(c^\dagger_{j,\uparrow} c_{j,\downarrow} - c^\dagger_{j,\downarrow} c_{j,\uparrow}) = B_y \sum_{i=1}^{L} \tfrac{1}{2}(M_j + i\eta_{\uparrow,j}\eta_{\downarrow,j}), \tag{8}$$

where $\eta_{\sigma,j} = i(c^\dagger_{\sigma,j} - c_{\sigma,j})$ are the other Majorana operators. Our density matrix renormalization group (DMRG) simulations indeed confirm that even a small field B_y reduces the fourfold degeneracy to a doublet of twofold (almost) degenerate states, with an energy difference which scales linearly with the system size L [53].

On the other hand, the fourfold degeneracy is protected against other local perturbations, including in particular a magnetic field in the (x, z) plane or a chemical potential: Our DMRG calculations indicate that the lifting induced by these perturbations is exponentially suppressed in the system length [53]. The protection of the degeneracy against some of these perturbations becomes apparent in the parafermionic language. Both the chemical potential and the magnetic field along the z axis conserve the total number of FPF modulo 4 and they thus feature a local expression also in terms of parafermions [53]. Our findings are consistent with the results of Refs. [54–56] in that the fully topologically protected part of the degeneracy (the part that cannot be lifted by symmetry-breaking local perturbations) is only twofold.

Phase diagram. Being an exactly solvable model, H_J allowed us to derive important analytical results such as the existence of the local order parameter M_j and the expression of the zero-energy parafermions in Eq. (7). The price we paid for this exact solvability is the rather complicated form of H_J in the fermionic basis, which in particular includes three-body interactions. Instead of searching for fine-tuned models that might realize Eqs. (4)–(6), we view this model as one representative of a much larger class of systems realizing parafermionic physics at low energies. In this spirit, the specific model H_J is not only crucial in that it allows us to fully understand the physics beyond any low-energy approximations, but also as a controlled starting point around which we now explore topologically equivalent models by smooth deformations of the Hamiltonian. As long as the gap is not closed, the system remains in the same topological phase and will feature the same topological properties. In particular, we consider the much more generic Hamiltonian

$$\bar{H}(U, V) = H^{(2)} + U[V(H^{(4)} + H^{(6)}) + (1 - V)\bar{H}^{(4)}], \tag{9}$$

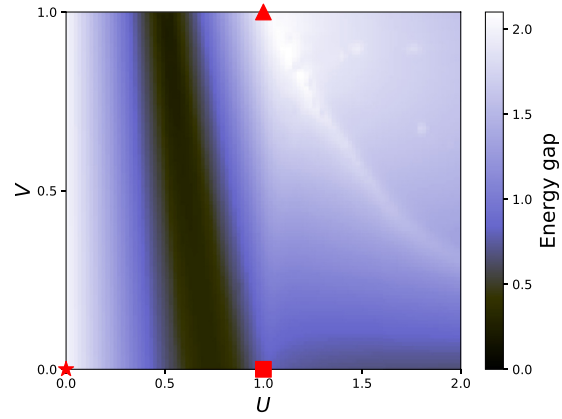

FIG. 1. Energy gap (units J) of $\bar{H}(U, V)$ as a function of U and V. The triangle, square, and star correspond to H_J, H_A, and $H^{(2)}$, respectively. DMRG simulations on 16 sites.

where the parameter U weights all interacting terms and V allows us to smoothly transform the three-body terms into simpler two-body terms with

$$\bar{H}^{(4)} = -J \sum_{\sigma,j} [c^\dagger_{\sigma,j} c_{\sigma,j+1}(-n_{-\sigma,j} - n_{-\sigma,j+1}) + c^\dagger_{\sigma,j} c^\dagger_{\sigma,j+1}(n_{-\sigma,j} - n_{-\sigma,j+1})] + \text{H.c.} \tag{10}$$

DMRG simulations on a chain with 16 sites reveal a gap closure in the region $U \sim 0.5$–0.7 (see Fig. 1). This defines two different phases: a "strongly interacting" (SI) one on the right and a "weakly interacting" (WI) one on the left. The original Hamiltonian H_J (triangle in Fig. 1) belongs to the SI phase and can be continuously deformed into $H_A = \bar{H}(1, 0)$ (square)—an Hamiltonian in the $\mathbb{Z}_4$ parafermionic phase *without* three-body interactions. Note that, away from the exactly solvable point H_J, Hamiltonians $\bar{H}$ in the SI phase feature an exact fourfold degeneracy (through out all the spectrum) only in the $L \to \infty$ limit.

Our numerics thus show that parafermionic physics can already be generated from occupation-dependent hopping and pairing terms. Experimentally, such conditional terms can be realized if, e.g., the hopping involves intermediate virtual states whose energies are tuned by the interaction. Somewhat simpler density-dependent hoppings have already been engineered in cold-atomic systems [57–59]. On more general grounds, however, any not strictly local interaction gives rise to occupation-dependent hoppings and pairings [60–62]. It would be most desirable to identify (quasi-)one-dimensional systems in which these occupation-dependent terms are of appreciable size—a challenging goal for future research that will also benefit from investigating the stability of the parafermionic phase under further modifications of the Hamiltonian.

Fermionic spectral function. From an experimental standpoint, a crucial (albeit not conclusive) signature of topological phases is the appearance of a zero-energy density of states at the ends of the topological chain. In general, the spin-averaged

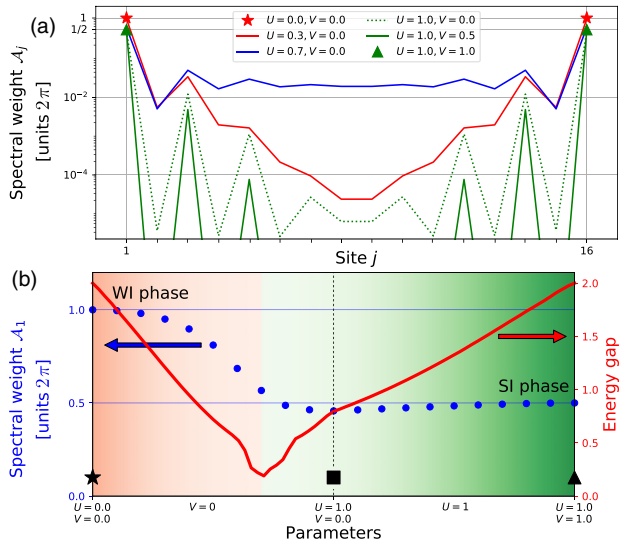

FIG. 2. (a) $\mathcal{A}_j$ for different points in the (U, V) parameter space. Green plots feature a dependence on the parity of the site j. (b) $\mathcal{A}_1$ (blue dots) along the straight paths in parameter space connecting $H^{(2)}$ (star), H_A (square), and H_J (triangle). The energy gap (units J) is shown in red to help in identifying the phase transition (here around $U \sim 0.7$) between the WI phase (red fade) and the SI one (green fade). DMRG simulations on 16 sites.

fermionic local spectral function at zero temperature reads

$$A_j(\omega) = 2\pi \sum_{\sigma,|\varphi\rangle} [\delta(\omega - E_\varphi + E_{\rm GS})|\langle\varphi|c^\dagger_{\sigma,j}|{\rm GS}\rangle|^2 + \delta(\omega + E_\varphi - E_{\rm GS})|\langle\varphi|c_{\sigma,j}|{\rm GS}\rangle|^2], \quad (11)$$

where $|\varphi\rangle$ are the eigenstates of the Hamiltonian with energies E_φ and $|{\rm GS}\rangle$ is the ground state the system is in [63].

At first, we focus on the exactly solvable Hamiltonian H_J. Denoting its four ground states with fixed FPF number m (modulo 4) by $|\psi_m\rangle$, one has that [53]

$$\sum_m |\langle\psi_m|c_{j\sigma}|\psi_l\rangle|^2 = (\delta_{j,1} + \delta_{j,L})\frac{1}{8} \quad (H = H_J), \quad (12)$$

for $l \in \{0, 1, 2, 3\}$ and $\sigma = \uparrow, \downarrow$. The same holds true for the creation operators. Focusing on energies below the gap, this immediately leads to a zero-energy peak $A_{1,L}(\omega) = \pi\delta(\omega)$ localized at the edges and to a vanishing spectral weight in the bulk, $A_j(\omega) = 0$ for $j \in \{2, \ldots, L-1\}$. This result is confirmed by DMRG simulations which also allowed us to move away from the exactly solvable point. In particular, in Fig. 2 we plot the spin-averaged spectral function integrated over the energy gap (EG) $\mathcal{A}_j = \int_{\rm EG} A_j(\omega)d\omega$ for different Hamiltonians. Interestingly, the spectral weight is robust with respect to variations of the parameters U and V as long as the system remains in the SI phase. The fermionic edge density of state remains indeed trapped at the edges and features only an exponentially suppressed leakage into the bulk. This is clearly displayed in Fig. 2(a). Note that the spectral weight within the gap has proven to be robust also with respect to other kinds of small perturbations such as magnetic fields (along *every* direction) and chemical potentials.

Figure 1 shows that a pronounced reduction of the interaction strength U eventually leads to a phase transition, located where the gap closes (in a finite system the gap reaches a minimum but remains finite). At this point the low-energy spectral weight is spread all over the chain, as testified by the blue plot in Fig. 2(a) computed for $U = 0.7$ and $V = 0$. Once the system enters the WI phase, the spectral weight localizes again at the edges but with an important difference: As clearly shown in Fig. 2(b), the low-energy spectral weight in the WI phase is twice the one in the SI one. The reason is that the WI phase features two couples of zero-energy Majoranas instead of a single pair of parafermions. The noninteracting and exactly solvable Hamiltonian $H^{(2)}$ (red star in Fig. 1), which belongs to the WI phase, can indeed be expressed as two decoupled Kitaev chains with four dangling edge Majoranas,

$$H^{(2)} = -Ji\sum_{j=1}^{L-1}[\tau_{\downarrow,j}\,\chi_{\downarrow,j+1} + \tau_{\uparrow,j}\,\chi_{\uparrow,j+1}], \quad (13)$$

where $\tau_{\sigma,j} = (\gamma_{-\sigma,j} + \eta_{\sigma,j})/\sqrt{2}$ and $\chi_{\sigma,j} = (\gamma_{\sigma,j} - \eta_{-\sigma,j})/\sqrt{2}$. Moreover, it is possible to show that the four ground states of $H^{(2)}$ satisfy [53]

$$\sum_m |\langle\phi_m|c_{j\sigma}|\phi_l\rangle|^2 = (\delta_{j,1} + \delta_{j,L})\frac{1}{4} \quad [H = H^{(2)}], \quad (14)$$

for $l \in \{0, 1, 2, 3\}$ and $\sigma = \uparrow, \downarrow$. The same holds true for the creation operator. This leads to a peak $A_{1,L}(\omega) = 2\pi\delta(\omega)$ whose weight is exactly twice the one found in the SI phase.

The zero-energy peak in the local spectral function, localized at the edges and with weight π in a system with a time-reversal symmetric Hamiltonian, provides therefore a robust signature of the SI phase and allows one to distinguish between the presence of its $\mathbb{Z}_4$ parafermionic modes and the two couples of Majoranas featured by the WI phase. The existence of the phase transition between SI and WI underlines once more that interparticle interactions play a crucial role for the emergence of zero-energy parafermions, as discussed also in Refs. [25,30,31,64].

Discussion and conclusions. In this Rapid Communication, we have introduced an exact mapping between $\mathbb{Z}_4$ parafermions and spinful fermions on a lattice. Despite the mapping's intrinsic nonlocality, we showed that certain local parafermionic Hamiltonians (conserving the total number of Fock parafermions modulo 4) can be mapped onto *local* fermionic Hamiltonians. This mapping thus allows for the systematic construction of interacting fermionic Hamiltonians on a lattice which feature zero-energy parafermionic modes.

In a first step, we focused on the exactly solvable fermionic model H_J. The $\mathbb{Z}_4$ symmetry of the parafermionic model translates into the combination of $\mathbb{Z}_2$ fermion parity and a $\mathbb{Z}_2$ spontaneously broken symmetry. This challenges the topological protection of the zero-energy modes obeying $\mathbb{Z}_4$ parafermionic algebra, whose exact expressions in terms of fermions are derived. The lack of topological protection is in agreement with other very recent findings [43,65] on similar lattice systems. We studied experimentally accessible

signatures of the $\mathbb{Z}_4$ parafermionic phase analytically, including in particular the fermionic density of states, and showed how it differs from other topological phases.

Importantly, the exactly solvable model H_J belongs to an entire topological phase, which we explored in a second step. This phase includes much simpler Hamiltonians, which are more suitable for numerical and experimental investigation while featuring the same topological properties of H_J.

Finally, the mapping we have introduced can be generalized to $\mathbb{Z}_p$ parafermions, which will be discussed elsewhere. In fact, as long as one chooses a suitable single-site basis, every local operator which conserves the total number of Fock parafermions modulo p can be expressed in terms of fermions without string factors.

Note added. Recently, we became aware of Ref. [65] that derives and studies a very similar model. The findings discussed in this reference are consistent with our results where they overlap.

Acknowledgments. A.C. and T.L.S. acknowledge financial support from the National Research Fund, Luxembourg, under Grant ATTRACT 7556175. T.M. is supported by Deutsche Forschungsgemeinschaft through the Emmy Noether Programme ME 4844/1-1 and through SFB 1143. The authors thank Hosho Katsura for useful discussions.

[1] M. Z. Hasan and C. L. Kane, Rev. Mod. Phys. **82**, 3045 (2010).
[2] X. Qi and S. Zhang, Rev. Mod. Phys. **83**, 1057 (2011).
[3] M. Leijnse and K. Flensberg, Semicond. Sci. Technol. **27**, 124003 (2012).
[4] C. Beenakker, Annu. Rev. Condens. Matter Phys. **4**, 113 (2013).
[5] C. Nayak, S. H. Simon, A. Stern, M. Freedman, and S. Das Sarma, Rev. Mod. Phys. **80**, 1083 (2008).
[6] A. Kitaev, Ann. Phys. **303**, 2 (2003).
[7] D. Aasen, M. Hell, R. V. Mishmash, A. Higginbotham, J. Danon, M. Leijnse, T. S. Jespersen, J. A. Folk, C. M. Marcus, K. Flensberg, and J. Alicea, Phys. Rev. X **6**, 031016 (2016).
[8] G. E. Volovik, *The Universe in a Helium Droplet* (Clarendon, Oxford, UK, 2003).
[9] A. Y. Kitaev, Phys. Usp. **44**, 131 (2001).
[10] J. Alicea, Rep. Prog. Phys. **75**, 076501 (2012).
[11] V. Mourik, K. Zuo, S. M. Frolov, S. R. Plissard, E. P. A. M. Bakkers, and L. P. Kouwenhoven, Science **336**, 1003 (2012).
[12] S. M. Albrecht, A. P. Higginbotham, M. Madsen, F. Kuemmeth, T. S. Jespersen, J. Nygård, P. Krogstrup, and C. M. Marcus, Nature (London) **531**, 206 (2016).
[13] R. M. Lutchyn, E. P. A. M. Bakkers, L. P. Kouwenhoven, P. Krogstrup, C. M. Marcus, and Y. Oreg, Nat. Rev. Mater. **3**, 52 (2018).
[14] Y. Oreg, G. Refael, and F. von Oppen, Phys. Rev. Lett. **105**, 177002 (2010).
[15] R. M. Lutchyn, J. D. Sau, and S. Das Sarma, Phys. Rev. Lett. **105**, 077001 (2010).
[16] M. T. Deng, S. Vaitiekenas, E. B. Hansen, J. Danon, M. Leijnse, K. Flensberg, J. Nygård, P. Krogstrup, and C. M. Marcus, Science **354**, 1557 (2016).
[17] S. Nadj-Perge, I. K. Drozdov, J. Li, H. Chen, S. Jeon, J. Seo, A. H. MacDonald, B. A. Bernevig, and A. Yazdani, Science **346**, 602 (2014).
[18] T.-P. Choy, J. M. Edge, A. R. Akhmerov, and C. W. J. Beenakker, Phys. Rev. B **84**, 195442 (2011).
[19] S. Nadj-Perge, I. K. Drozdov, B. A. Bernevig, and A. Yazdani, Phys. Rev. B **88**, 020407 (2013).
[20] J. Klinovaja, P. Stano, A. Yazdani, and D. Loss, Phys. Rev. Lett. **111**, 186805 (2013).
[21] M. Ruby, F. Pientka, Y. Peng, F. von Oppen, B. W. Heinrich, and K. J. Franke, Phys. Rev. Lett. **115**, 197204 (2015).
[22] B. E. Feldman, M. T. Randeria, J. Li, S. Jeon, Y. Xie, Z. Wang, I. K. Drozdov, B. A. Bernevig, and A. Yazdani, Nat. Phys. **13**, 286 (2017).
[23] A. Hutter and D. Loss, Phys. Rev. B **93**, 125105 (2016).
[24] C. P. Orth, R. P. Tiwari, T. Meng, and T. L. Schmidt, Phys. Rev. B **91**, 081406(R) (2015).
[25] Y. Vinkler-Aviv, P. W. Brouwer, and F. von Oppen, Phys. Rev. B **96**, 195421 (2017).
[26] F. Zhang and C. L. Kane, Phys. Rev. Lett. **113**, 036401 (2014).
[27] J. Klinovaja, A. Yacoby, and D. Loss, Phys. Rev. B **90**, 155447 (2014).
[28] C. Fleckenstein, N. Traverso Ziani, and B. Trauzettel, arXiv:1810.00764.
[29] C. J. Pedder, T. Meng, R. P. Tiwari, and T. L. Schmidt, Phys. Rev. B **94**, 245414 (2016).
[30] C. J. Pedder, T. Meng, R. P. Tiwari, and T. L. Schmidt, Phys. Rev. B **96**, 165429 (2017).
[31] J. Klinovaja and D. Loss, Phys. Rev. Lett. **112**, 246403 (2014).
[32] M. Barkeshli and X.-L. Qi, Phys. Rev. X **4**, 041035 (2014).
[33] D. J. Clarke, J. Alicea, and K. Shtengel, Nat. Commun. **4**, 1348 (2013).
[34] N. H. Lindner, E. Berg, G. Refael, and A. Stern, Phys. Rev. X **2**, 041002 (2012).
[35] Y. Alavirad, D. Clarke, A. Nag, and J. D. Sau, Phys. Rev. Lett. **119**, 217701 (2017).
[36] C. Chen and F. J. Burnell, Phys. Rev. Lett. **116**, 106405 (2016).
[37] A. Vaezi, Phys. Rev. B **87**, 035132 (2013).
[38] A. Vaezi, Phys. Rev. X **4**, 031009 (2014).
[39] M.-S. Vaezi and A. Vaezi, arXiv:1706.01192.
[40] M. Barkeshli, C.-M. Jian, and X.-L. Qi, Phys. Rev. B **87**, 045130 (2013).
[41] L. H. Santos and T. L. Hughes, Phys. Rev. Lett. **118**, 136801 (2017).
[42] F. Iemini, C. Mora, and L. Mazza, Phys. Rev. Lett. **118**, 170402 (2017).
[43] L. Mazza, F. Iemini, M. Dalmonte, and C. Mora, Phys. Rev. B **98**, 201109 (2018).
[44] A. S. Jermyn, R. S. K. Mong, J. Alicea, and P. Fendley, Phys. Rev. B **90**, 165106 (2014).
[45] P. Fendley, J. Stat. Mech. (2012) P11020.
[46] P. Fendley, J. Phys. A **47**, 075001 (2014).
[47] J. Alicea and P. Fendley, Annu. Rev. Condens. Matter Phys. **7**, 119 (2016).

[48] R. S. K. Mong, D. J. Clarke, J. Alicea, N. H. Lindner, and P. Fendley, J. Phys. A **47**, 452001 (2014).
[49] E. M. Stoudenmire, D. J. Clarke, R. S. K. Mong, and J. Alicea, Phys. Rev. B **91**, 235112 (2015).
[50] K. Meichanetzidis, C. J. Turner, A. Farjami, Z. Papić, and J. K. Pachos, Phys. Rev. B **97**, 125104 (2018).
[51] L. Mazza, J. Viti, M. Carrega, D. Rossini, and A. De Luca, Phys. Rev. B **98**, 075421 (2018).
[52] E. Cobanera and G. Ortiz, Phys. Rev. A **89**, 012328 (2014).
[53] See Supplemental Material at http://link.aps.org/supplemental/10.1103/PhysRevB.98.201110 for more detailed descriptions of the mapping and of the model's fermionic properties.
[54] L. Fidkowski and A. Kitaev, Phys. Rev. B **83**, 075103 (2011).
[55] A. M. Turner, F. Pollmann, and E. Berg, Phys. Rev. B **83**, 075102 (2011).
[56] N. Bultinck, D. J. Williamson, J. Haegeman, and F. Verstraete, Phys. Rev. B **95**, 075108 (2017).
[57] O. Jürgensen, F. Meinert, M. J. Mark, H.-C. Nägerl, and D.-S. Lühmann, Phys. Rev. Lett. **113**, 193003 (2014).
[58] F. Meinert, M. J. Mark, K. Lauber, A. J. Daley, and H.-C. Nägerl, Phys. Rev. Lett. **116**, 205301 (2016).
[59] S. Baier, M. J. Mark, D. Petter, K. Aikawa, L. Chomaz, Z. Cai, M. Baranov, P. Zoller, and F. Ferlaino, Science **352**, 201 (2016).
[60] S. Kivelson, W.-P. Su, J. R. Schrieffer, and A. J. Heeger, Phys. Rev. Lett. **58**, 1899 (1987).
[61] J. Hirsch, Physica C (Amsterdam) **158**, 326 (1989).
[62] J. Hirsch, Physica B (Amsterdam) **199-200**, 366 (1994).
[63] For the numerical computation of the spectral function in presence of degeneracy, we select the ground state with odd fermion parity and with the lower expectation value of M_1. Different choices would not have modified the results we presented, though.
[64] J. Klinovaja and D. Loss, Phys. Rev. B **90**, 045118 (2014).
[65] A. Chew, D. F. Mross, and J. Alicea, Phys. Rev. B **98**, 085143 (2018).